Journal of Colloid and Interface Science 640 (2023) 510–520

Contents lists available at ScienceDirect

Journal of Colloid and Interface Science

journal homepage: www.elsevier.com/locate/jcis

Deciphering the adaption of bacterial cell wall mechanical integrity and turgor to different chemical or mechanical environments

Rui Han [a], Xi-Qiao Feng [b], Waldemar Vollmer [c], Paul Stoodley [d,e], Jinju Chen [a,*]

[a] School of Engineering, Newcastle University, Newcastle upon Tyne NE1 7RU, UK
[b] Institute of Biomechanics and Medical Engineering, Department of Engineering Mechanics, Tsinghua University, Beijing 100084, China
[c] Centre for Bacterial Cell Biology, Biosciences Institute, Newcastle University, Newcastle upon Tyne NE2 4AX, UK
[d] Department of Microbial Infection and Immunity and the Department of Orthopaedics, The Ohio State University, Columbus, OH 43210, United States
[e] National Centre for Advanced Tribology at Southampton (nCATS), National Biofilm Innovation Centre (NBIC), Mechanical Engineering, University of Southampton, Southampton S017 1BJ, UK

GRAPHICAL ABSTRACT

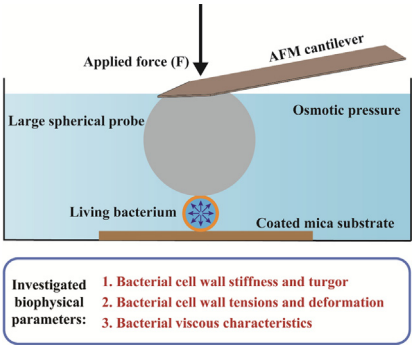

ARTICLE INFO

Article history:
Received 28 December 2022
Revised 16 February 2023
Accepted 19 February 2023
Available online 23 February 2023

Keywords:
Bacterial cell wall stiffness and turgor
Bacterial cell wall tensions and deformation
Bacterial viscous properties
Atomic force microscopy (AFM)
Chemical and mechanical stimuli

ABSTRACT

Bacteria adapt the mechanical properties of their cell envelope, including cell wall stiffness, turgor, and cell wall tension and deformation, to grow and survive in harsh environments. However, it remains a technical challenge to simultaneously determine these mechanical properties at a single cell level. Here we combined theoretical modelling with an experimental approach to quantify the mechanical properties and turgor of *Staphylococcus epidermidis*. It was found that high osmolarity leads to a decrease in both cell wall stiffness and turgor. We also demonstrated that the turgor change is associated with a change in the viscosity of the bacterial cell. We predicted that the cell wall tension is much higher in deionized (DI) water and it decreases with an increase in osmolality. We also found that an external force increases the cell wall deformation to reinforce its adherence to a surface and this effect can be more significant in lower osmolarity. Overall, our work highlights how bacterial mechanics supports survival in harsh environments and uncovers the adaption of bacterial cell wall mechanical integrity and turgor to osmotic and mechanical challenges.

© 2023 The Author(s). Published by Elsevier Inc. This is an open access article under the CC BY license (http://creativecommons.org/licenses/by/4.0/).

1. Introduction

Cellular-scale processes of bacteria, for example growth, cell division and motility, depend on the mechanical properties and

* Corresponding author.
E-mail address: jinju.chen@ncl.ac.uk (J. Chen).

https://doi.org/10.1016/j.jcis.2023.02.100
0021-9797/© 2023 The Author(s). Published by Elsevier Inc.
This is an open access article under the CC BY license (http://creativecommons.org/licenses/by/4.0/).

interactions of the cell envelope [1–4]. As a polymeric meshwork surrounding the cell, the bacterial cell wall mainly consists of peptidoglycan (PG), a network of long glycan chains connected by stretchable peptides. PG protects bacteria from osmotic lysis and maintains the cell shape and mechanical integrity [5–10]. The PG also helps to accommodate the selective transport of compounds across the cell envelope. It undergoes changes during growth and division, and transfers signals from the environment into the cell [11]. These functions require that both the architecture [12] and mechanical properties of the bacteria and its cell envelope are dynamic and adaptive to the environment [13,14]. The osmotic pressure difference between the cytoplasm and extracellular environment (turgor) affects the possible mechanical cell deformation [4]. The mechanical properties of the cell envelope contribute to the structural integrity and survival of cells under conditions of external forces, adhesion force, and other environmental conditions, i.e., pH levels [15], ionic strength [16], temperature [17], and the nature of the surrounding materials [18–22]. Therefore, we need to determine the mechanical properties and turgor of the bacterial cells to gain better understanding of bacterial behaviours.

Atomic force microscopy (AFM) is specifically well suited to visualize the cell morphology in the growth and division process of cells (e.g., bacteria, yeast and eukaryotic cells), and to quantify the interaction forces between cells and the substrate [23–27]. The AFM-based indentation technique has been applied to measure the mechanical properties of bacteria, such as Young's modulus (apparent cell modulus), bacterial cell wall stiffness, and turgor [6,13,14,27–31], using a cantilever tip to probe the cellular elastic response under an externally applied force. For different bacteria, the apparent cell moduli measured by AFM range from 0.05 MPa to 769 MPa [3], which depends on the fixation method [26], temperature, chemical environments, and other factors. For example, Francius *et al.* [32] found that antibiotic agents such as lysostaphin decrease the bacterial cell wall stiffness for *Staphylococcus aureus*. This study demonstrated that cell wall structure changes were correlated with major differences in cell wall nanomechanical properties, which involved complicated mechanisms such as the digestion of peptidoglycan by lysostaphin and eventually leads to the formation of osmotically fragile cells. Cerf *et al* [17] have found that an exposure at 45 °C caused cell membrane damage in *E. coli* DH5α cells, which caused the apparent cell modulus to increase 2-fold compared to cells kept at 37 °C. In all these investigations, the apparent cell modulus was determined by assuming the bacterial cell as a solid structure based on the Hertz or Sneddon models. Very recently, Han and Chen *et al.* [27,33] further developed the Sneddon model by introducing the effects of the sample size and tip angles and used this modified model to determine the apparent cell modulus of *Staphylococcus epidermidis*.

Mechanically individual bacterial cells can be considered and modelled as rigid wall, liquid-filled shell structures with turgor [7,8]. Both, bacterial cell wall stiffness and turgor are important for bacterial survival and adaptation. A few approaches have been proposed to determine these two key parameters. For instance, Yao *et al.* [34] proposed a theoretical method to describe the mechanical behavior of spherical bacteria, and derived the relationship between the indentation depth of the samples and turgor. Arnold *et al* [35] reported another theoretical model, using a function of the indentation depth caused by the AFM tip and the cell wall deformation, based on the local deformation of rob-shaped bacteria. Deng *et al.* [29] studied intact and bulging *E. coli* cells to separate the contributions of the cell wall and turgor to the cell wall stiffness and found evidence to support power-law stress stiffening in *E. coli* cell wall. In addition, Zhang *et al.* [14] developed an explicit expression to explain the relation between turgor and rod-shaped cell wall elasticity through AFM and finite element method (FEM). Recently, we proposed a method to determine the bacterial cell wall stiffness and turgor simultaneously by using modified Reissner model and inverse finite element analysis [27]. However, there is a lack of studies investigating the osmotic effect on cell wall stiffness, turgor, cell wall tensions and cell wall deformation [4].

In the present work, we adapted a mathematical model, initially developed for engineered capsulates [36–38] to decipher the mechanical properties (cell wall stiffness, turgor, cell wall tensions and deformation) of a representative Gram-positive spherical bacterium, *S. epidermidis*, using AFM fitted with a large spherical probe. We propose a biophysical mechanism to explain how these key mechanical properties will be altered by the turgor and how they may correlate with cell wall deformation.

2. Materials and methods

2.1. Theoretical model

The deformation analysis method for a liquid-filled spherical shell structure with internal pressure is based on the analysis of Feng and Yang [39], Lardner and Pujara [40], and others [41–44]. The cell wall is assumed as a homogenous, isotropic, and linear elastic material. Fig. 1(a) shows the sample compressed by a large flat plate. The wall can be divided into the contact and non-contact regions. The governing equations for the contact and non-contact regions are given in ESI*. The radius of the sample is inflated from the initial radius r_0 to r_i and the thickness of the cell wall t. Spherical coordinates (r, θ, φ) were used for the inflated sphere before contact, and cylindrical coordinates (ρ, θ, η) were used after the deformation of the sphere, as seen in Fig. 1(a). At a given force, the deformation of the inflated sphere depends on wall stiffness (E) and Poisson's ratio (ν), turgor (P_0) and initial stretch ratio (λ_0), as seen in Fig. S1-S3 in supporting information. The governing differential equations were applied separately to contact regions and non-contact regions. These equations with their boundary conditions (see supporting information) can be solved by the Runge-Kutta method, using the MTLAB (MathWorks Inc.) ode45 solver [43]. To solve this multivariant and multi-objective optimization problem, the "fminsearch" function in MATLAB was employed (based on a simplex search method, which uses sum of errors for optimization) [45]. The flowchart for solving governing equations was presented in Fig. 1(b).

2.2. AFM measurements and macro-compression tests

All AFM measurements were performed with a Flex-Bio AFM instrument (Nanosurf, Switzerland) was mounted on an Axio Observer D1 inverted microscope (Carl Zeiss, Jena, Germany). Monolithic silicon cantilevers CP-qp-CONT-BSG, each fitted with a 5 μm spherical probe were purchased from Apex Probes (Apex Probes ltd., Bracknell, UK), with a spring constant of about 0.1 m/N. We used the thermal tune method to calibrate the spring constants of all cantilevers, which were in a range of 0.1–0.12 m/N. The cantilevers were cleaned in a UV/ozone cleaner (BioForce Nanoscience, Inc., Ames, IA) and the deflection sensitivity was measured on a mica piece. All force measurements were performed as in our previous work [27]. The bacterial culture (*Staphylococcus epidermidis* FH8 cells) and the details of immobilizing the samples onto the coated mica piece (71855–15-10, Sigma-Aldrich) can be found in [27]. Seven different osmolarity environments for bacteria were considered, including deionized (DI) water, 0.15 M, 0.75 M, 1.5 M phosphate-buffered saline (PBS, D1408, Sigma-Aldrich), and 0.1 M, 0.5 M, 1 M $CaCl_2$ solutions (C5670, $\geq$ 96.0 %, Sigma-Aldrich). The procedure makes sure that the samples could not dry. For bacterial samples, 36 cells were measured for each condition, and three tests were performed for each cell, thereby provid-

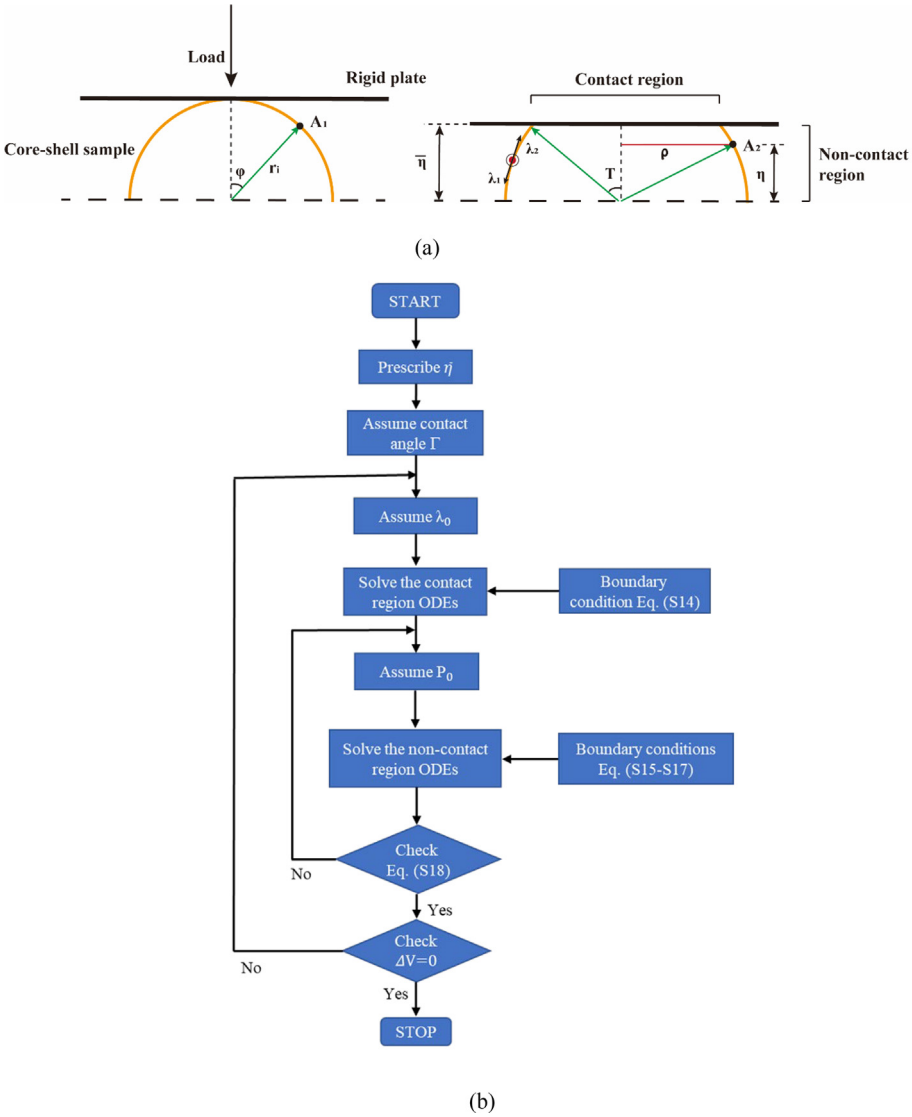

Fig. 1. (a) Schematic of the indentation test of an inflated spherical shell structure compressed by a large plate before and after deformation. (b) The flowchart for solving governing equations of the model, where the equations were detailed in supporting information.

ing 108 force–indentation depth curves. AFM measurements would be completed within 2 h and the samples were still viable during the measurements [27].

The compression tests on the inflatable butyl rubber balls were purchased from Yuansheng Sports Company, Wuxi, China. They were inflated with different pressure (10 kPa and 15 kPa, as measured by a pressure gauge) and then compressed between two large rigid plates using AGS-X 100 kN universal testing machine (Shimadzu Corporation, Japan). These compression tests will be used to validate the theoretical model under the ambient condition. The maximum deformation depth of 60 mm (35 % relative deformation) with a loading rate of 20 mm/s was applied in all tests, and at least 5 measurements were made.

2.3. Finite element method (FEM)

In principle, when the characteristic size of the spherical probe is sufficiently large compared to the bacterial cell, the AFM measurements can be approximately represented by the model described in Section 2.1. To reveal the required size ratio of the spherical probe and the bacterium, we employed FEM to simulate the indentation of bacteria using both a rigid plate and spherical probes of different diameters (1–10 times of the bacterial size). To improve the computational efficiency, a two-dimensional (2D) axisymmetric model was developed, using commercial software ABAQUS/Standard 6.18. In the FE models, as shown in Fig. 2, the interaction between the indenter and the sample was normal hard and tangential frictionless contact. CAX4RH elements (A 4-node bilinear axisymmetric quadrilateral, hybrid, constant pressure, reduced integration, hourglass control) were used in all simulations. Displacement-controlled loading was applied. In the FE model here, the bacterium diameter of 600 nm was chosen based on experimental measurements (see Fig. S4 and Table S1 in supporting information) and bacterial cell wall thickness of 30 nm was chosen based on what was reported [27]. Poisson's ratio of the cell wall was fixed as 0.49 [27]. To mimic the turgor in a bacterial cell, the fluid cavity module was utilized [46].

3. Results and discussions

3.1. Experimental and numerical results for model validation

The material parameters of the inflated butyl rubber balls used in the theoretical model were listed in Table 1. The theoretical

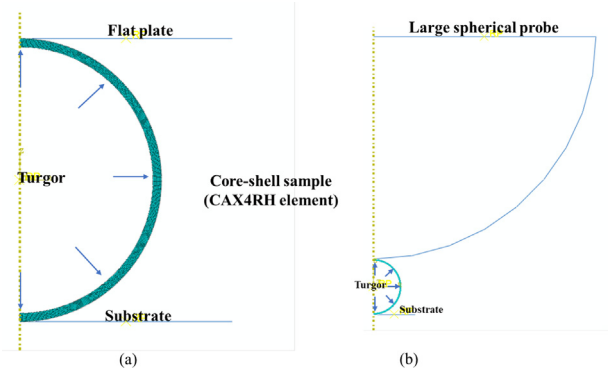

Fig. 2. FE models of AFM indentation tests of a representative spherical bacterium using (a) a flat plate and (b) a large spherical probe with a diameter of 6000 nm (10 times of the bacterial size).

model predictions agreed well with the experimental data (R-squ are $\geq$ 0.98), as seen in Fig. 3a. The force-relative deformation curves based on FE simulations for indenting a representative bacterium using a flat plate and various spherical probes (1–10 times size of bacteria) were presented in Fig. 3(b). It was found that a spherical probe can be simplified as a flat plate if its size is over 8 times larger than the sample (difference $\leq$ 5 %), especially when the deformation is below 35 % (the max deformation ratio in this study). Therefore, the analytical model was applicable to the indentation of a bacterium (with diameter of 600 nm) using the big spherical probe (with diameter of 5 μm) which was the case in this study.

3.2. Bacterial cell wall stiffness and initial stretch ratio

The indentation tests were repeated at the center of individual cells. A few representative force–depth curves and the fitting curves are displayed in Fig. 4(a)-(b). We first determined the two vital mechanical parameters, i.e., initial stretch ratio λ_0 and cell wall stiffness E, by fitting force–deformation curves from the numerical simulations. In all calculations, we took the Poisson's ratio of the cell wall as 0.49, which is common for biological samples [14], and the same diameter (600 nm) and wall thickness (30 nm) were used as the input parameters in the analytical model because different media used here had little effect on bacterial size (Table S1 in supporting information) [48]. A wide range of simulations with various initial stretch ratios and cell wall stiffnesses were computed when the fitting process is the best (R-square = 0.998). In addition, Fig. 4(c)-(d) compared the cell wall stiffness and the initial stretch ratio of *S. epidermidis* in DI water, 0.15 M, 0.75 M, 1.5 M PBS, and 0.1 M, 0.5 M, 1 M $CaCl_2$. Both parameters were predicted to decrease with increasing medium osmolarity (See Table S2 in supporting information), which was consistent with a previous study by Stenson [49]. There was a significant difference of cell wall stiffness between DI water and other osmotic mediums, specifically, the cell wall of *S. epidermidis* was about twice as stiff in DI water compared to PBS and $CaCl_2$. This is likely because a high osmotic condition may compact the cell wall to enhance its stiffness [50] as illustrated in Fig. 4(e). Furthermore, the stiffness was slightly larger in $CaCl_2$ than PBS at the same osmolarity, possibly because a lower pH of 5.0 (compared to 7.4 in PBS) and Ca^{2+} ions contributed to the structure and integrity of the cell wall [51,52]. On the other hand, there was no obvious difference in the initial stretch ratio (1.4–1.6 in various conditions) while the parameter has a largest value, 1.59, in DI water.

3.3. Turgor change during deformation

The variations of turgor with respect to the relative deformation in different environments were shown in Fig. 5(a)-(b). It is seen that the turgor showed a nonlinear (parabolic) increase with respect to the imposed deformation. However, an approximately linear relation occurred at a deformation smaller than 20 %, and the turgor initially increased slowly and then increased rapidly. In addition, at zero relative deformation, the turgor was not equal to 0 but 2.12 MPa in 0.15 M PBS because of the presence of the initial stretch ratio. The difference of turgor, $\sim$ 60 %, with and without the mechanical stimuli, and the initial turgor of bacteria in different osmotic conditions as well, indicating that the combined chemical and mechanical stimuli, in general, turgor decreases but to less extent (Fig. 5(c)-(d)). A significant difference in turgor was found for *S. epidermidis* under different osmotic conditions, and the turgor for the samples in PBS and $CaCl_2$ dropped by about 30 % or 60 % compared to bacteria in DI water. Both the turgor and cell stiffness decreased when the external osmotic pressure increased [50]. However, the turgor in PBS was larger than that of in $CaCl_2$, even though the osmolarity of PBS (280–315 mOsm/L) and 0.1 M $CaCl_2$ (300 mOsm/L) was almost similar, this might because K^+ ions in PBS play an active role in the recovery of the turgor [55]. By reducing the osmolarity of the medium, the cell wall stiffness and turgor of bacterial cells increase, in agreement with Deng *et al.* [29], who showed that the cell wall stiffness of *E. coli* correlates with the turgor and proposed a stress-stiffening response as a mechanism to limit shape-changes under high osmotic pressure. A turgor-mediated increase in stiffness was also reported in yeast [28] and *streptococci* [13]. In all cases, turgor increased with the deformation and the percentage of the turgor increase at a given deformation was similar.

Fig. 6(a) showed a strong correlation between the turgor and the cell wall stiffness of *S. epidermidis* in DI water, PBS, and $CaCl_2$ solutions. The ratio of cell wall stiffness and turgor (slope k) increased with the increase in osmolarity. This suggests that the cell wall stiffness and turgor of *S. epidermidis* are more sensitive to a medium with stronger ionic strength [13,56]. Our findings are important for understanding how bacterial cell shape and growth may vary in different osmotic environments [57,58]. In the simulations of Gram-negative bacterium, *Klebsiella pneumoniae*, Feng's group predicted a linear relation in the log–log plot for the normalized cell wall stiffness and normalized turgor [14]. In our results in Fig. 5(b), a similar linear relation has been observed for *S. epidermidis* in $CaCl_2$ solutions and partially for *S. epidermidis* in PBS at higher turgor. However, the linear relation in the log–log plot does not exist for *S. epidermidis* in DI water in Fig. 6(b). The bacterial cell wall stiffness values, determined using AFM fitted with a large spherical probe in this work, agree with what was determined using a pyramid probe in our previous study [27]. Furthermore, turgor is also consistent with other studies for

Table 1
Material parameters of the inflated butyl rubber balls.

Radius: r_0 (mm)	Thickness: t (mm)	Initial stretch ratio:λ_0	Initial internal pressure: P_0 (kPa)	Young's modulus [47]: E (GPa)	Poisson's ratio [47]: v
77.5	1.0	1.13	10	0.06	0.49
77.5	1.0	1.22	15	0.06	0.49

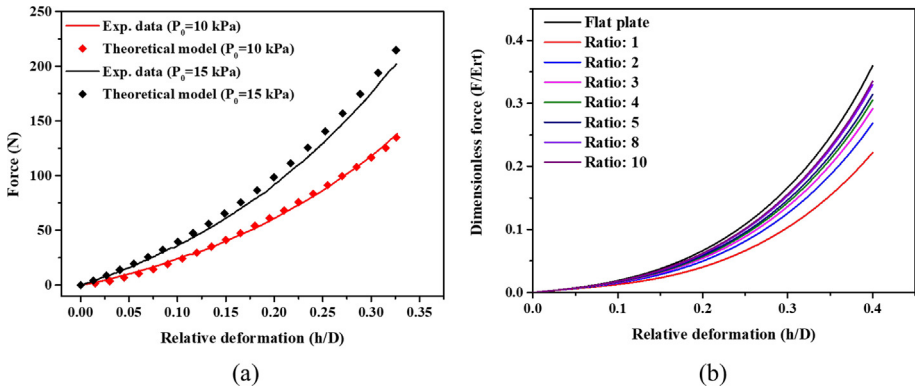

Fig. 3. (a) Comparison of indentation force-relative deformation curves of the inflated rubber balls with different internal pressures obtained from the experimental measurements and the predictive model, n = 20. (b) Force-relative deformation curves for probes of different sizes. Where size ratio of the spherical probe over the bacterium was 1 – 10.

the Gram-positive bacterium *Staphylococcus aureus* [4,27,29,30] and our previous study [27].

3.4. Tensions and deformation in the bacterial cell wall

Using the theoretical model, the bacterial cell wall tensions, here defined by the principal stress resultants per unit length of the deformed surface, were obtained at 35 % relative deformation as shown in Fig. 7(a)-(b). The meridian and circumferential tension T_1 and T_2 in the cell wall were not uniform but increased with the contact angle φ, and the cell wall tension in the circumferential direction T_2 was always larger than that in the deformed meridional T_1. On this basis, the possible rupturing position would be located on the cell's equator due to the symmetry of the loading condition, if the friction of the contact area was neglected [41]. Fig. 7(c)-(d) showed the comparison of the cell wall tensions, T_1 and T_2, of *S. epidermidis* in DI water, 0.15 M, 0.75 M, 1.5 M PBS, and 0.1 M, 0.5 M, 1 M $CaCl_2$ solutions. A significant difference was found in cell wall tensions between DI water, PBS and $CaCl_2$ solution, and cell wall tensions dropped about 12 % and 18 % in PBS and $CaCl_2$ respectively, compared to DI water. The maximum cell wall tensions with respect to the relative deformation in different environments (Fig. 8(e)-(f)) shows a nonlinear (parabolic) increase of the tensions with the deformation. In addition, the cell wall tensions were not 0 at zero deformation due to the turgor. Fig. 8(g)-(h) displayed the initial cell wall tensions of *S. epidermidis* in different osmotic environments, and the effect of osmolarity on these initial tensions was similar with the maximum tensions (Fig. 8(c)-(d)). Accurate determination of cell wall tensions helps to understand diverse cell biological processes that involve shaping and remodeling of cell wall [61,62].

Cell wall deformation induced by external mechanical and chemical stimuli can affect cell growth and shape [22,57,58,63–65], and adhesion [6–8,10,66,67]. Fig. 8(a)-(d) illustrated the representative calculated deformed profiles of the samples in DI water, and 0.15 M, 0.75 M or 1.5 M PBS. It is seen that the non-contact region could be significantly stretched to maintain a constant enclosed volume during the deformation. There was a significant difference in the deformed profile for *S. epidermidis* under different osmotic conditions, and the dimensionless lateral and vertical deformation decreased with the increase in the medium osmolarity. Similar observations were also found for $CaCl_2$ with different concentrations (see Fig. S5 in supporting information). The changes imply that the cells are under low tensile stress in physiological osmolarity, and less stretched than in hypotonic environment [13]. On the other hand, the deformation can increase the adhesion (pair-wise molecular interaction) as it brings more molecules [66] through the cell envelope, closer to substratum surface. Associated cell wall deformation could allow bacteria to sense the presence of a substratum surface and their adhering state through changes in the bacterial cell wall tensions to which membrane-located sensory molecules could trigger phenotypic and genotypic responses in biofilms [68]. More specifically, there was a larger contact area of *S. epidermidis* in DI water compared to other conditions, indicating that *S. epidermidis* did easier adhere to a substratum surface in DI water. The external force increased the cell wall deformation to increase the adherence to the surface and such effect could be more significant in lower osmolarity.

3.5. Viscous behaviors in different environments

For bacterial cell mechanics, the viscoelastic characteristics arise from the combined polymeric nature of bacterial cell wall and cytoplasm. As expected, we observed hysteresis in the loading–unloading force–displacement curves due to the viscoelasticity of bacteria (Fig. S6(a)-(b) in supporting information). Interestingly, the displacement did not return to zero during unloading when the force reduced to zero. This may be due to the irreversible polymer structure arrangement in the cytoplasm, because the cell wall PG can recover its structure after removing the load [52]. Numerical integration of the force–displacement curves allowed us to determine both energy loss and the elastic energy (Fig. 9(a)-(b)). The energy loss, elastic energy and total work during the AFM measurements were all the highest for bacteria in DI water, followed by PBS and $CaCl_2$. These parameters are proportional to the viscous, elastic, and apparent moduli at given deformation, respectively, suggesting that the change of turgor is also associated with the viscous modulus. It also suggests that the apparent moduli for bacteria in those seven media should follow the same order, in agreement with our results (Fig. 6(b)). On the other hand, the ratio of energy loss over the elastic energy was proportional to the ratio of viscous modulus over elastic modulus. This ratio is below 1 for more solid-like materials. For *S. epidermidis* measured here, this ratio was about 0.29 in DI water, and the value increased with the osmolarity of medium, being higher in $CaCl_2$ solution than in PBS (Fig. 9(c)), and the values were close to our previous work using AFM fitted with a pyramid probe [27].

It has been found that cells accumulate some specific compatible solutes under osmotic stress [69,70]. The intracellular viscosity has been associated with the thermal stability of biomolecules [71] and the metabolic state of the cell (active growth or dormancy) [72], and it might allow cells to adapt to temperature changes and the availability of nutrients [73]. Such 'viscoadaptation' in response to osmolarity and temperature may enable *S. epidermidis*

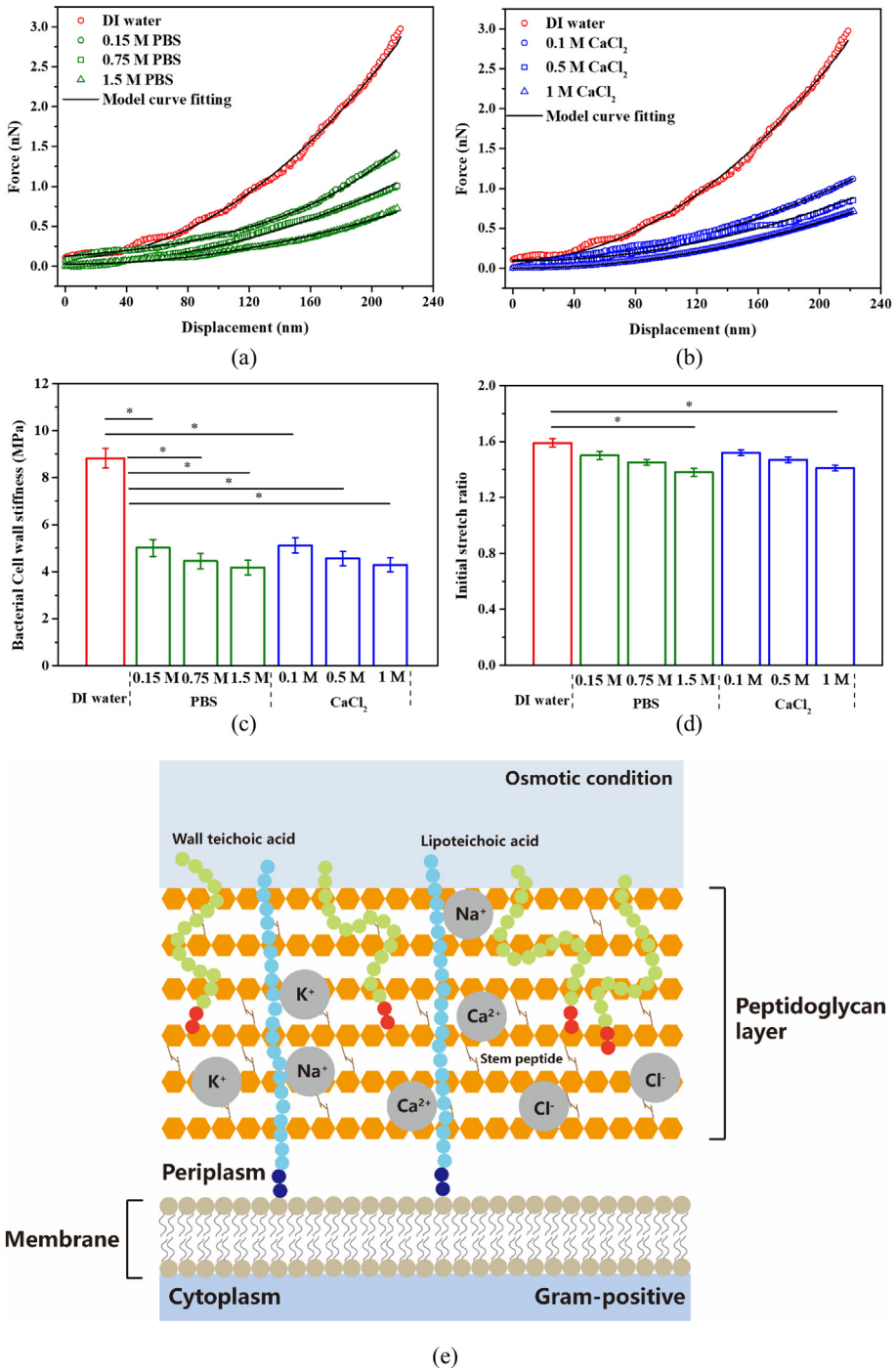

Fig. 4. (a)-(b) Comparisons of the experimental and numerical force–displacement curves at a 35 % relative deformation (Diameter: 600 nm, thickness: 30 nm, Poisson's ratios: 0.49) in (a) DI water and various PBS, (b) DI water and $CaCl_2$ solutions. (c)-(d) Cell wall stiffness and the initial stretch ratio of *S. epidermidis* under different osmotic conditions, $^*p < 0.05$, n = 108. (e) Cartoon depicting the cell wall of Gram-positive bacteria. Divalent ions interact with the PG layer and teichoic acids. Teichoic acids have a particularly strong affinity for divalent cations and have been proposed to provide a capacity to store ions [53,54].

to thrive in the high osmotic environment of the skin and adapt to survival in the blood when entering a surgical site and causing periprosthetic joint and other surgical site infections.

4. Conclusions

This work has demonstrated that the simultaneous determination of bacterial cell wall stiffness, turgor and cell wall tension can be achieved from a single AFM indentation test through mathematical modelling. The proposed analytical model was validated by our experimental results of engineering materials. When it was applied to bacteria, we obtained values of cell wall stiffness and turgor of *S. epidermidis* in various chemical environments in which were consistent with what have been recently reported using AFM fitted with a pyramid probe [27]. We demonstrated that the bacterial cell wall stiffness and cell wall tension decreased with the osmotic pressure, likely due to altered interactions between cations and the PG-teichoic acid complex in the cell wall. We have

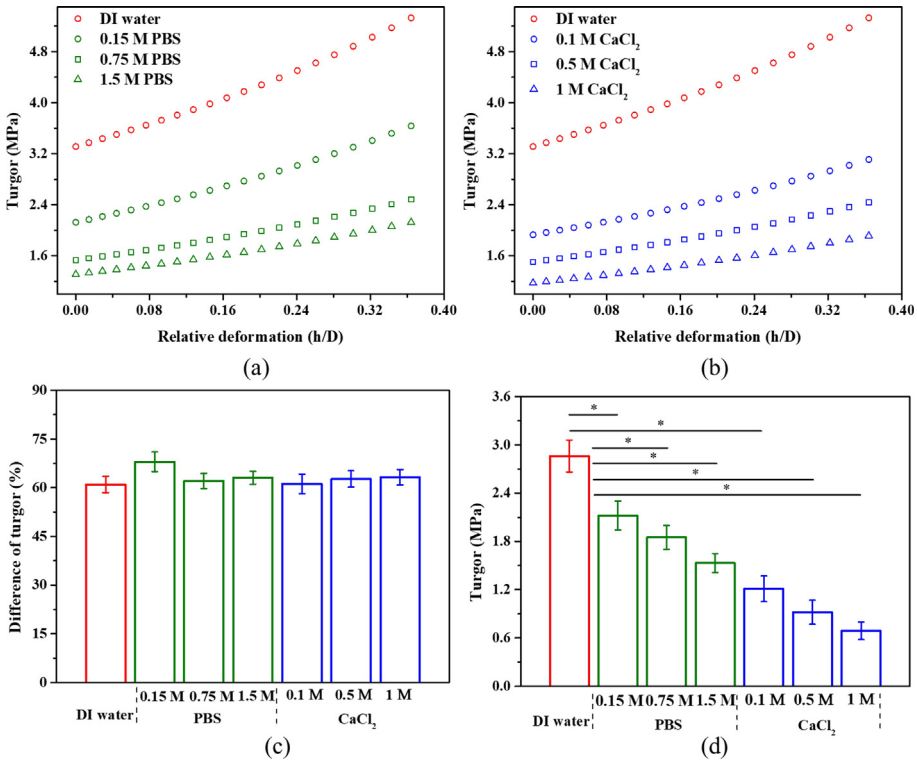

Fig. 5. (a)-(b) Representative curves of turgor versus relative deformation under varying osmotic environments. (c) The turgor difference for *S. epidermidis* in different osmotic conditions at zero and 35 % deformation. (d) The initial turgor for *S. epidermidis* under different osmotic conditions at zero deformation, $^{*}p < 0.05$, n = 108.

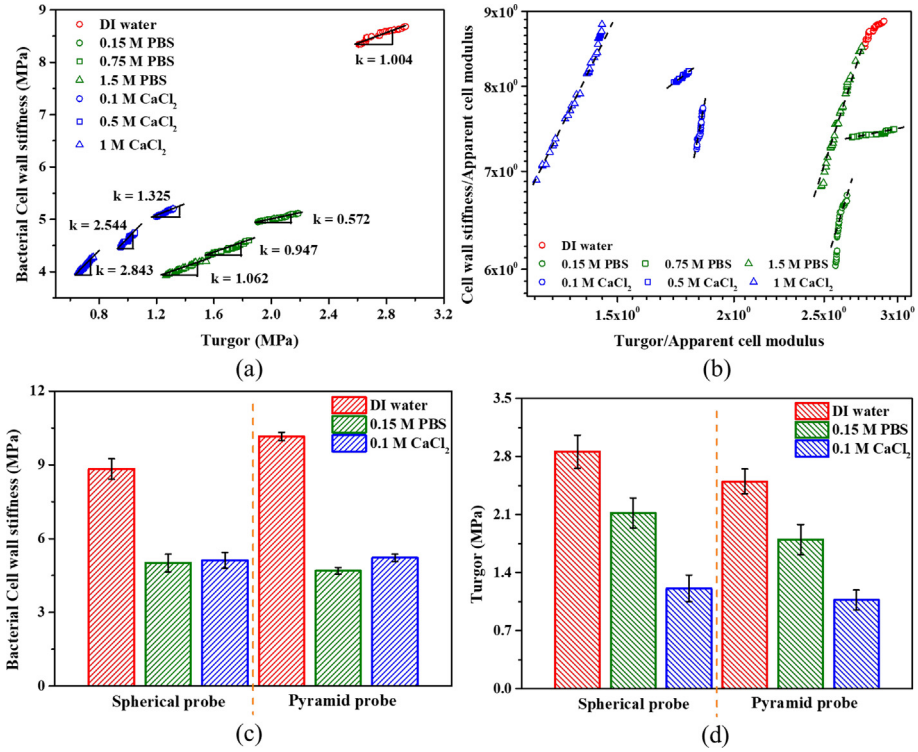

Fig. 6. (a) Correlation between the turgor and the cell wall stiffness under different osmotic conditions. (b) The log–log plot of normalized the turgor and the cell wall stiffness against the apparent cell modulus (determined by modified Sneddon model [59,60]) under different osmotic conditions. (c)-(d) Comparisons of bacterial cell wall stiffness and turgor when using a large spherical probe and a pyramid probe, where the results for pyramid probe were taken from [27], n = 108.

also discovered that bacteria in higher osmolarity appeared to be more viscous. Such 'viscoadaptation' in response to osmolarity and temperature by *S. epidermidis* may be an important strategy to survival in the high osmotic environment of skin and blood to cause infections. The external mechanical force increased the apparent turgor. Our method cab be used in future work to eluci-

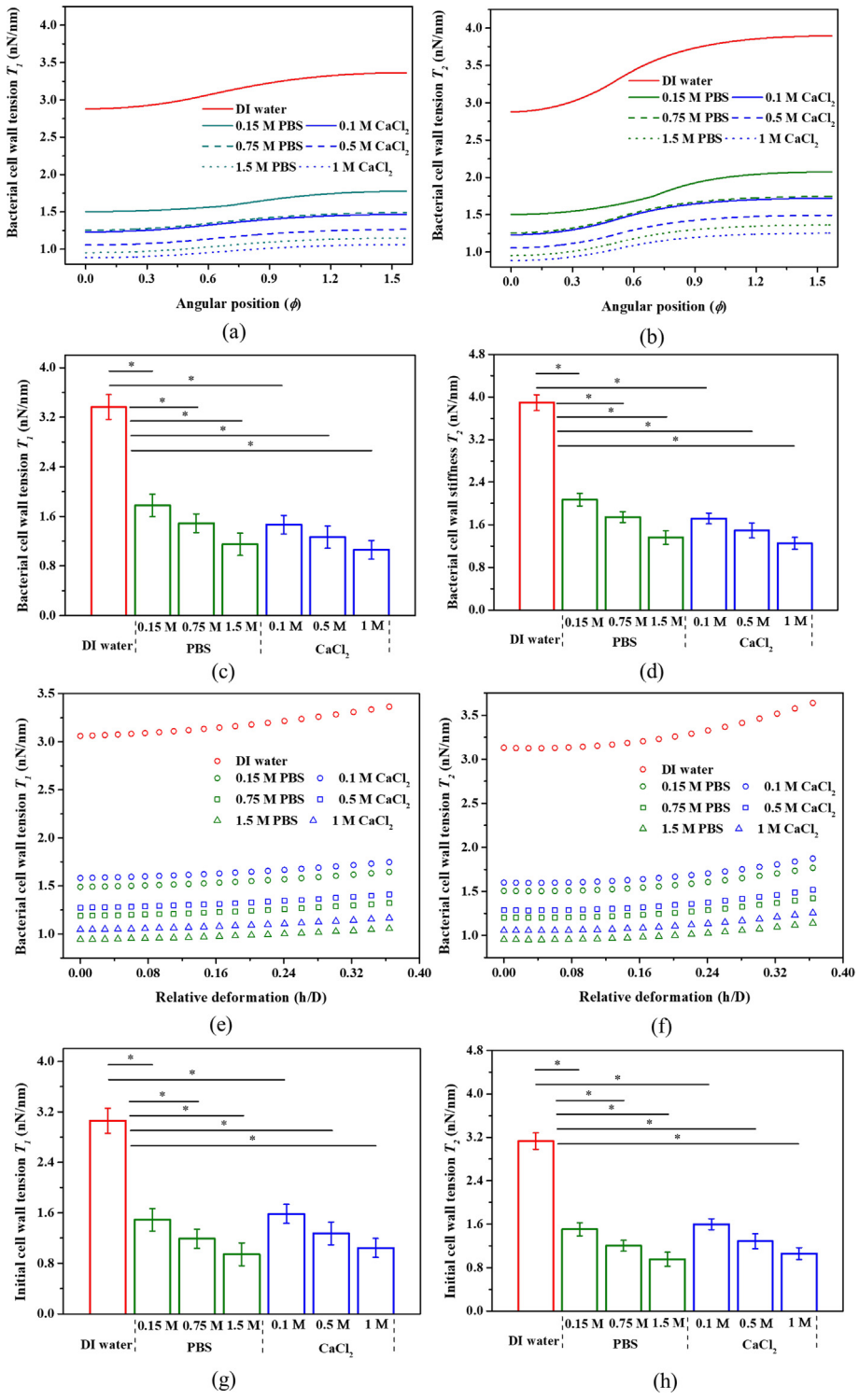

Fig. 7. (a)-(b) Comparison of the cell wall tensions with angular position φ at the relative deformation of 35 %. (c)-(d) The maximum cell wall tensions, T_1 and T_2, for *S. epidermidis* under different osmotic conditions, $^*p < 0.05$, n = 108. (e)-(f) Bacterial cell wall tensions, T_1 and T_2, varied with the deformation under different osmotic conditions. (g)-(h) The initial cell wall tensions, T_1 and T_2, for *S. epidermidis* under different osmotic conditions, $^*p < 0.05$, n = 108.

date how bacteria can modify their cell wall mechanical integrity and turgor in response to survival from osmotic challenges (chemical stimuli) or mechanical deformation (mechanical stimuli).

Data availability statement

The data is available upon request.

CRediT authorship contribution statement

Rui Han: Conceptualization, Methodology, Software, Validation, Visualization, Writing – original draft, Writing – review & editing. **Xi-Qiao Feng:** Supervision, Writing – original draft, Writing – review & editing. **Waldemar Vollmer:** Supervision, Writing – original draft, Writing – review & editing. **Paul Stoodley:** Supervision,

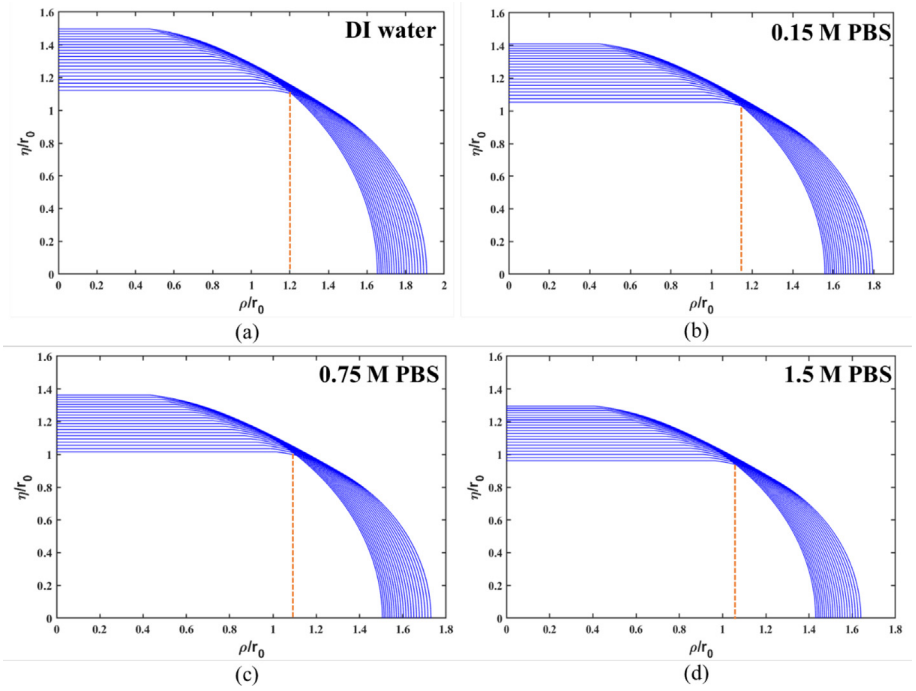

Fig. 8. Representative of geometric profile of *S. epidermidis* during deformation under different osmotic conditions (where ρ is the lateral radius of the deformed bacterial cell and r_0 is initial bacterial radius): (a) DI water, (b) 0.15 M PBS, (c) 0.75 M PBS, (d) 1.5 M PBS.

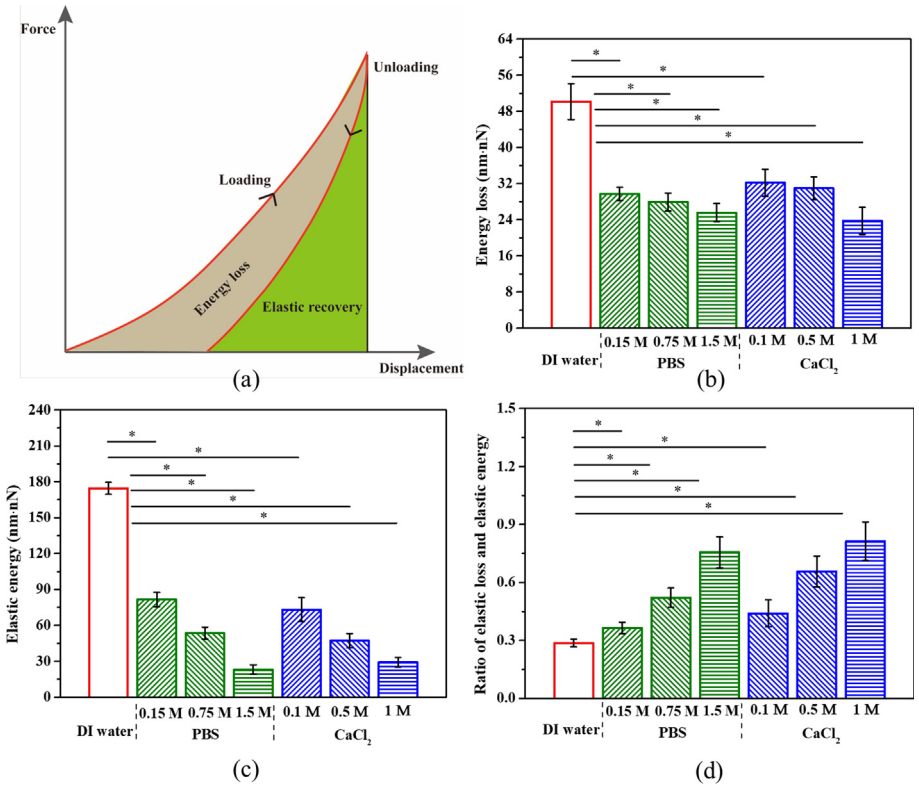

Fig. 9. (a) Schematic of the energy loss and elastic recovery of bacterial cells in a loading–unloading process under different osmotic conditions. (b)-(c) Comparison of energy loss and elastic energy, (d) the ratio of energy loss and elastic energy. $^*p < 0.05$, n = 108.

Writing – original draft, Writing – review & editing. **Jinju Chen:** Conceptualization, Methodology, Investigation, Validation, Supervision, Project administration, Funding acquisition, Writing - original draft, Writing - review & editing.

Data availability

Data will be made available on request.

Declaration of Competing Interest

The authors declare that they have no known competing financial interests or personal relationships that could have appeared to influence the work reported in this paper.

Acknowledgements

J. Chen acknowledges funding from the Engineering and Physical Sciences Research Council (EP/R025606/1; EP/V049615/1). W. Vollmer was supported by the UKRI Strategic Priorities Fund (EP/T002778/1) and the BBSRC (BB/W013630/1). R. Han acknowledges the PhD scholarship from Chinese Scholarship Council and Newcastle University. We are very grateful for very constructive comments from Prof. Henk J. Busscher and Dr. Fei Pan. Prof. NS Jakubovic is acknowledged for providing the bacteria used for this study. We thank Ross Laws, Tracey Davey and Yufeng Zhu for their support on SEM imaging. We thank Paul Scott for technical support of Shimadzu test machine.

Appendix A. Supplementary material

Supplementary data to this article can be found online at https://doi.org/10.1016/j.jcis.2023.02.100.

References

[1] J.V. Holtje, Growth of the stress-bearing and shape-maintaining murein sacculus of Escherichia coli, Microbiol. Mol. Biol. R. 62 (1) (1998) 181–203.
[2] L. Furchtgott, N.S. Wingreen, K.C. Huang, Mechanisms for maintaining cell shape in rod-shaped Gram-negative bacteria, Mol. Microbiol. 81 (2) (2011) 340–353.
[3] H.H. Tuson, G.K. Auer, L.D. Renner, M. Hasebe, C. Tropini, M. Salick, W.C. Crone, A. Gopinathan, K.C. Huang, D.B. Weibel, Measuring the stiffness of bacterial cells from growth rates in hydrogels of tunable elasticity, Mol. Microbiol. 84 (5) (2012) 874–891.
[4] E.R. Rojas, K.C. Huang, Regulation of microbial growth by turgor pressure, Curr. Opin. Microbiol. 42 (2018) 62–70.
[5] T. Das, P.K. Sharma, B.P. Krom, H.C. van der Mei, H.J. Busscher, Role of eDNA on the adhesion forces between Streptococcus mutans and substratum surfaces: influence of ionic strength and substratum hydrophobicity, Langmuir 27 (16) (2011) 10113–10118.
[6] Y. Chen, W. Norde, H.C. van der Mei, H.J. Busscher, Bacterial cell surface deformation under external loading, MBio 3 (6) (2012). e00378–12.
[7] Y. Chen, A.K. Harapanahalli, H.J. Busscher, W. Norde, H.C. van der Mei, Nanoscale cell wall deformation impacts long-range bacterial adhesion forces on surfaces, Appl. Environ. Microbiol. 80 (2) (2014) 637–643.
[8] J. Li, H.J. Busscher, J.J.T.M. Swartjes, Y. Chen, A.K. Harapanahalli, W. Norde, H.C. van der Mei, J. Sjollema, Residence-time dependent cell wall deformation of different Staphylococcus aureus strains on gold measured using surface-enhanced-fluorescence, Soft Matter 10 (38) (2014) 7638–7646.
[9] V. Carniello, A.K. Harapanahalli, H.J. Busscher, H.C. van der Mei, Adhesion force sensing and activation of a membrane-bound sensor to activate nisin efflux pumps in Staphylococcus aureus under mechanical and chemical stresses, J. Colloid Interf. Sci. 512 (2018) 14–20.
[10] V. Carniello, B.W. Peterson, J. Sjollema, H.J. Busscher, H.C. van der Mei, Surface enhanced fluorescence and nanoscopic cell wall deformation in adhering Staphylococcus aureus upon exposure to cell wall active and non-active antibiotics, Nanoscale 10 (23) (2018) 11123–11133.
[11] J.J. Thwaites, N.H. Mendelson, Mechanical behaviour of bacterial cell walls, Adv. Microb. Physiol. 32 (1991) 173–222.
[12] L. Pasquina-Lemonche, J. Burns, R.D. Turner, S. Kumar, R. Tank, N. Mullin, J.S. Wilson, B. Chakrabarti, P.A. Bullough, S.J. Foster, J.K. Hobbs, The architecture of the Gram-positive bacterial cell wall, Nature 582 (7811) (2020) 294–297.
[13] R.S. Dover, A. Bitler, E. Shimoni, P. Trieu-Cuot, Y. Shai, Multiparametric AFM reveals turgor-responsive net-like peptidoglycan architecture in live streptococci, Nat. Commun. 6 (2015) 7193.
[14] H.X. Zhang, H.B. Wang, J.J. Wilksch, R.A. Strugnell, M.L. Gee, X.Q. Feng, Measurement of the interconnected turgor pressure and envelope elasticity of live bacterial cells, Soft Matter 17 (8) (2021) 2042–2049.
[15] S. Zheng, M. Bawazir, A. Dhall, H.-E. Kim, L. He, J. Heo, G. Hwang, Implication of surface properties, bacterial motility, and hydrodynamic conditions on bacterial surface sensing and their initial adhesion, Front. Bioeng. Biotechnol. 9 (2021).
[16] C.B. Volle, M.A. Ferguson, K.E. Aidala, E.M. Spain, M.E. Nunez, Quantitative changes in the elasticity and adhesive properties of Escherichia coli ZK1056 prey cells during predation by bdellovibrio bacteriovorus 109J, Langmuir 24 (15) (2008) 8102–8110.
[17] A. Cerf, J.C. Cau, C. Vieu, E. Dague, Nanomechanical properties of dead or alive single-patterned bacteria, Langmuir 25 (10) (2009) 5731–5736.
[18] Y. Zhu, G. McHale, J. Dawson, S. Armstrong, G. Wells, R. Han, H. Liu, W. Vollmer, P. Stoodley, N. Jakubovics, J. Chen, Slippery liquid-like solid surfaces with promising antibiofilm performance under both static and flow conditions, ACS Appl. Mater. Interfaces 14 (5) (2022) 6307–6319.
[19] S.J. Yunyi Cao, Xiaolong Tan, Leon Bowen, Yufeng Zhu, Jack Dawson, Rui Han, John Exton, Hongzhong Liu, Glen McHale, Nicholas Jakubovics, Jinju Chen, Anti-wetting and anti-fouling performances of different lubricant-infused slippery surfaces, Langmuir 36, 45 (2020) 13396–13407.
[20] F. Pan, S. Altenried, M.D. Liu, D. Hegemann, E. Bulbul, J. Moeller, W.W. Schmahl, K. Maniura-Weber, Q. Ren, A nanolayer coating on polydimethylsiloxane surfaces enables a mechanistic study of bacterial adhesion influenced by material surface physicochemistry, Mater Horizons 7 (1) (2020) 93–103.
[21] H. Straub, C.M. Bigger, J. Valentin, D. Abt, X.H. Qin, L. Eberl, K. Maniura-Weber, Q. Ren, Bacterial adhesion on soft materials: passive physicochemical interactions or active bacterial mechanosensing?, Adv Healthc. Mater. 8 (8) (2019).
[22] N. Kandemir, W. Vollmer, N.S. Jakubovics, J. Chen, Mechanical interactions between bacteria and hydrogels, Sci. Rep. 8 (1) (2018) 10893.
[23] G.T. Charras, M.A. Horton, Single cell mechanotransduction and its modulation analyzed by atomic force microscope indentation, Biophys. J. 82 (6) (2002) 2970–2981.
[24] L. Mikoliunaite, A. Makaraviciute, A. Suchodolskis, A. Ramanaviciene, Y. Oztekin, A. Stirke, G. Jurkaite, M. Ukanis, G. Carac, P. Cojocaru, Atomic force microscopy study of living Baker's yeast cells, Adv. Sci. Lett. 4 (2011) 368–376.
[25] A. Suchodolskis, A. Stirke, A. Timonina, A. Ramanaviciene, Baker's yeast transformation studies by atomic force microscopy, Adv. Sci. Lett. 4 (2011) 171–173.
[26] I. Morkvėnaitė-Vilkončienė, A. Ramanavičienė, A. Ramanavičius, Atomic force microscopy as a tool for the investigation of living cells, Medicina 49 (4) (2013) 25.
[27] R. Han, W. Vollmer, J.D. Perry, P. Stoodley, J. Chen, Simultaneous determination of the mechanical properties and turgor of a single bacterial cell using atomic force microscopy, Nanoscale 14 (33) (2022) 12060–12068.
[28] J. Arfsten, S. Leupold, C. Bradtmoller, I. Kampen, A. Kwade, Atomic force microscopy studies on the nanomechanical properties of Saccharomyces cerevisiae, Colloids Surf. B Biointerfaces 79 (1) (2010) 284–290.
[29] Y. Deng, M.Z. Sun, J.W. Shaevitz, Direct measurement of cell wall stress stiffening and turgor pressure in live bacterial cells, Phys. Rev. Lett. 107 (15) (2011).
[30] R.G. Bailey, R.D. Turner, N. Mullin, N. Clarke, S.J. Foster, J.K. Hobbs, The interplay between cell wall mechanical properties and the cell cycle in Staphylococcus aureus, Biophys. J. 107 (11) (2014) 2538–2545.
[31] M. Li, D. Dang, L. Liu, N. Xi, Y. Wang, Atomic force microscopy in characterizing cell mechanics for biomedical applications: a review, Ieee T Nanobiosci. 16 (6) (2017) 523–540.
[32] G. Francius, O. Domenech, M.P. Mingeot-Leclercq, Y.F. Dufrene, Direct observation of Staphylococcus aureus cell wall digestion by Lysostaphin, J. Bacteriol. 190 (24) (2008) 7904–7909.
[33] R. Han, J.J. Chen, A modified Sneddon model for the contact between conical indenters and spherical samples, J. Mater. Res. 36 (8) (2021) 1762–1771.
[34] X. Yao, J. Walter, S. Burke, S. Stewart, M.H. Jericho, D. Pink, R. Hunter, T.J. Beveridge, Atomic force microscopy and theoretical considerations of surface properties and turgor pressures of bacteria, Colloid Surface B 23 (2–3) (2002) 213–230.
[35] M. Arnoldi, M. Fritz, E. Bauerlein, M. Radmacher, E. Sackmann, A. Boulbitch, Bacterial turgor pressure can be measured by atomic force microscopy, Phys. Rev. E 62 (1) (2000) 1034–1044.
[36] M.W. Keller, N.R. Sottos, Mechanical properties of microcapsules used in a self-healing polymer, Exp. Mech. 46 (2006) 725–733.
[37] K. Bando, K. Ohba, Y. Oiso, Deformation analysis of microcapsules compressed by two rigid parallel plates, J. Biorheol. 27 (1) (2013) 18–25.
[38] N. Kumar, A. DasGupta, On the contact problem of an inflated spherical hyperelastic membrane, Int. J. Nonlin Mech. 57 (2013) 130–139.
[39] W.H.Y.W.W. Feng, On the contact problem of an inflated spherical nonlinear membrane, J. Appl. Mech. 40 (1) (1973) 209–214.
[40] T.J. Lardner, P. Pujara, XII - Compression of Spherical Cells, in: S. Nemat-Nasser (Ed.), Mechanics Today, Pergamon1980, pp. 161–176.
[41] K.K. Liu, D.R. Williams, B.J. Briscoe, Compressive deformation of a single microcapsule, Phys. Rev. E Stat. Phys. Plasmas Fluids Relat Interdiscip. Topics 54 (6) (1996) 6673–6680.

[42] A.E. Smith, K.E. Moxham, A.P.J. Middelberg, On uniquely determining cell–wall material properties with the compression experiment, Chem. Eng. Sci. 53 (23) (1998) 3913–3922.
[43] C.X. Wang, L. Wang, C.R. Thomas, Modelling the mechanical properties of single suspension-cultured tomato cells, Ann. Bot. 93 (4) (2004) 443–453.
[44] W.-H. Hsu, Y.-H. Chien, H.-Y. Tsai, Experimental and modeling analysis of the cell-wall fracture of nannochloropsis oculata, J. Mech. 36 (6) (2020) 789–797.
[45] X.F. Wang, R. Han, J. Tao, T.L. Han, G.M. Zhu, J.N. Tang, N.X. Han, F. Xing, Identification of mechanical parameters of urea-formaldehyde microcapsules using finite-element method, Compos. Part B-Eng. 158 (2019) 249–258.
[46] M. Smith, ABAQUS/Standard User's Manual, Version 6.14, Dassault Systèmes Simulia Corp, United States, 2014.
[47] A.K. Sharma, B. Bhattacharya, Parameter estimation of butyl rubber aided with dynamic mechanical analysis for numerical modelling of an air-inflated torus and experimental validation using 3D-laser Doppler vibrometer, J. Low Frequency Noise Vibration Active Control 38 (2) (2019) 296–311.
[48] L.A. Onyango, R.H. Dunstan, J. Gottfries, C. von Eiff, T.K. Roberts, Effect of low temperature on growth and ultra-structure of Staphylococcus spp, PLoS One 7 (1) (2012) e29031–e.
[49] J.D. Stenson, Investigating the Mechanical Properties of Yeast Cells, The University of Birmingham, School of Engineering, 2008.
[50] R.E. Marquis, Salt-induced contraction of bacterial cell walls, J. Bacteriol. 95 (3) (1968) 775–781.
[51] F. Gaboriaud, S. Bailet, E. Dague, F. Jorand, Surface structure and nanomechanical properties of Shewanella putrefaciens bacteria at two pH values (4 and 10) determined by atomic force microscopy, J. Bacteriol. 187 (11) (2005) 3864–3868.
[52] R.J. Smith, Calcium and Bacteria, in: R.K. Poole (Ed.), Advances in Microbial Physiology, Academic Press, 1995, pp. 83–133.
[53] C. Weidenmaier, A. Peschel, Teichoic acids and related cell-wall glycopolymers in Gram-positive physiology and host interactions, Nat. Rev. Microbiol. 6 (4) (2008) 276–287.
[54] T. Kern, M. Giffard, S. Hediger, A. Amoroso, C. Giustini, N.K. Bui, B. Joris, C. Bougault, W. Vollmer, J.-P. Simorre, Dynamics characterization of fully hydrated bacterial cell walls by solid-state NMR: evidence for cooperative binding of metal ions, J. Am. Chem. Soc. 132 (31) (2010) 10911–10919.
[55] A.M. Whatmore, R.H. Reed, Determination of turgor pressure in Bacillus subtilis: a possible role for K+ in turgor regulation, J. Gen. Microbiol. 136 (12) (1990) 2521–2526.
[56] D. Szatmari, P. Sarkany, B. Kocsis, T. Nagy, A. Miseta, S. Barko, B. Longauer, R.C. Robinson, M. Nyitrai, Intracellular ion concentrations and cation-dependent remodelling of bacterial MreB assemblies, Sci. Rep. 10 (1) (2020) 12002.
[57] S. al-Mosleh, A. Gopinathan, C.D. Santangelo, K.C. Huang, E.R. Rojas, Feedback linking cell envelope stiffness, curvature, and synthesis enables robust rod-shaped bacterial growth, Proceedings of the National Academy of Sciences 119 (41) (2022) e2200728119.
[58] A. Miguel, M. Zietek, H. Shi, A. Sueki, L. Maier, J. Verheul, T.d. Blaauwen, D.V. Valen, A. Typas, K.C. Huang, Modulation of bacterial cell size and growth rate via activation of a cell envelope stress response, bioRxiv (2022) 2022.07.26.501648.
[59] J.J. Chen, Nanobiomechanics of living cells: a review, Interface Focus 4 (2) (2014) 20130055.
[60] R. Han, X.F. Wang, G.M. Zhu, N.X. Han, F. Xing, Investigation on viscoelastic properties of urea-formaldehyde microcapsules by using nanoindentation, Polym. Test. 80 (2019) 106146.
[61] M.M. Kozlov, L.V. Chernomordik, Membrane tension and membrane fusion, Curr. Opin. Struct. Biol. 33 (2015) 61–67.
[62] E.R. Rojas, K.C. Huang, J.A. Theriot, Homeostatic cell growth is accomplished mechanically through membrane tension inhibition of cell-wall synthesis, Cell Syst. 5 (6) (2017) 578–590.e6.
[63] A. Amir, F. Babaeipour, D.B. McIntosh, D.R. Nelson, S. Jun, Bending forces plastically deform growing bacterial cell walls, Proc. Natl. Acad. Sci. 111(16) (2014) 5778–5783.
[64] P.P. Navarro, A. Vettiger, V.Y. Ananda, P.M. Llopis, C. Allolio, T.G. Bernhardt, L.H. Chao, Cell wall synthesis and remodelling dynamics determine division site architecture and cell shape in Escherichia coli, Nat. Microbiol. 7 (2022) 1621–1634.
[65] F. Si, B. Li, W. Margolin, S.X. Sun, Bacterial growth and form under mechanical compression, Sci Rep-Uk 5 (1) (2015) 11367.
[66] V. Carniello, B.W. Peterson, H.C. van der Mei, H.J. Busscher, Physico-chemistry from initial bacterial adhesion to surface-programmed biofilm growth, Adv. Colloid Interface Sci. 261 (2018) 1–14.
[67] V. Carniello, B.W. Peterson, H.C. van der Mei, H.J. Busscher, Role of adhesion forces in mechanosensitive channel gating in Staphylococcus aureus adhering to surfaces, npj Biofilms Microbiomes 6 (1) (2020) 31.
[68] H.J. Busscher, H.C. van der Mei, How do bacteria know they are on a surface and regulate their response to an adhering state?, PLoS Pathog 8 (1) (2012) e1002440.
[69] M.S. da Costa, H. Santos, E.A. Galinski, An overview of the role and diversity of compatible solutes in Bacteria and Archaea, in: G. Antranikian (Ed.), Biotechnology of Extremophiles, Springer, Berlin Heidelberg, Berlin, Heidelberg, 1998, pp. 117–153.
[70] M.I. Calderón, C. Vargas, F. Rojo, F. Iglesias-Guerra, L.N. Csonka, A. Ventosa, J.J. Nieto, Complex regulation of the synthesis of the compatible solute ectoine in the halophilic bacterium Chromohalobacter salexigens DSM 3043T, Microbiology 150 (Pt 9) (2004) 3051–3063.
[71] A. Cuecas, J. Cruces, J.F. Galisteo-López, X. Peng, J.M. Gonzalez, Cellular viscosity in prokaryotes and thermal stability of low molecular weight biomolecules, Biophys. J. 111 (4) (2016) 875–882.
[72] B.R. Parry, I.V. Surovtsev, M.T. Cabeen, C.S. O'Hern, E.R. Dufresne, C. Jacobs-Wagner, The bacterial cytoplasm has glass-like properties and is fluidized by metabolic activity, Cell 156 (1–2) (2014) 183–194.
[73] L.B. Persson, V.S. Ambati, O. Brandman, Cellular control of viscosity counters changes in temperature and energy availability, Cell 183 (6) (2020) 1572–1585.e16.